

# Low-threshold photonic crystal laser

Marko Lončar, Tomoyuki Yoshie, Axel Scherer

*Department of Electrical Engineering, California Institute of Technology, MS 136-93, Pasadena,  
CA 91125*

Pawan Gogna, Yueming Qiu

*In Situ Technology and Experiments Systems Section, Jet Propulsion Laboratory, MS 302-306,  
4800 Oak Grove Drive, Pasadena, CA 91109*

## Abstract

We have fabricated photonic crystal nanocavity lasers, based on a new high-quality factor design that incorporates fractional edge dislocations. Lasers with InGaAsP quantum well active material emitting at 1550nm were optically pumped with 10ns pulses, and lase at threshold pumping powers below 220 $\mu$ W, the lowest reported for photonic crystal lasers. Polarization characteristics, and lithographic tuning properties were found to be in excellent agreement with theoretical predictions.

The quest for a compact nano-cavity laser, with high quality factor (Q) and small mode volume ( $V_{mode}$ ), has been a central part of research in the field of integrated optics. Such high-Q nanocavities could allow for control of interaction between the light and matter, and is ideally suited for the exploration of cavity quantum electrodynamics phenomena as well as the control over spontaneous emission. Photonic crystals<sup>1</sup>, and planar photonic crystals in particular<sup>2</sup> (PPC), are promising manufacturable geometries for the integration of compact optical nano-devices with waveguides, modulators and detectors. So far there have been several reports on room temperature lasing in PPC nanocavities<sup>3-7</sup>, and more recently, new high-Q cavity designs based on modification of 2-D photonic crystals have been proposed<sup>4,8</sup>. In this letter we report the experimental application of one of these designs. The cavities are based on fractional edge dislocations<sup>8</sup>, and are used for the construction of a low-threshold laser in which the high field from the laser surrounds a void for chemical sensing or strong coupling to atomic light sources.

The structure we use for our laser is the simplest triangular lattice single defect cavity containing a fractional edge dislocation. The cavity consists of a defect hole that is smaller than surrounding holes which define the photonic crystal mirror. The row that contains the defect hole is elongated by moving two photonic crystal half-planes a fraction of a lattice constant apart in the  $\Gamma X$  direction, with a dislocation parameter  $p$  (Figure 1). We have shown earlier<sup>8</sup> that by tuning this  $p$ -parameter, Q factors of single defect cavities can be significantly improved, and reach Q values of over 10,000 when  $p/a = 10\%$  ( $a$  is the lattice constant). These high Q values are obtained while maintaining a very small mode volume of  $V_{mode} \approx 0.1(\lambda/2)^3$ . The cavity used in our laser was originally designed for cavity QED experiments and nano-spectroscopy, where strong-coupling between material introduced into the high field region of the cavity is to be investigated. Atomic light sources can be placed in the small hole in the center of the 2-D photonic crystal cavity, where the optical cavity field intensity is the strongest. However, it is clear that the presence of a hole at the point of maximum field intensity is not necessarily desirable in low-threshold laser designs, since the overlap with the gain region is decreased. Therefore, we expect even better cavity designs

to yield further improvements over the performance of the lasers described here.

Our structures are fabricated in InGaAsP quantum well material. Metalorganic chemical vapor deposition (MOCVD) was used to grow the active laser structure on an InP substrate. Optical gain is provided by four  $9nm$  thick, compressively strained, quantum wells with an electronic bandgap at  $E_g = 1.55\mu m$ , separated by  $20nm$  thick InGaAsP barriers ( $E_g = 1.22\mu m$ ). This active material is placed in the center of a  $330nm$  thick InGaAsP slab ( $E_g = 1.22\mu m$ ), with  $1\mu m$  thick sacrificial InP layer underneath the slab. A InGaAs etch stop is introduced above the InP substrate, and the active quaternary material is designed to operate at  $\lambda = 1.55\mu m$ . Because of the compressive strain, the coupling is the strongest to the TE polarized modes of the slab. This is desirable since in triangular lattice PPC the bandgap is larger for TE-polarized light. An etch mask consisting of  $40nm$  Au evaporated on top of  $100nm$  SiON, deposited using PCVD. The fabrication process starts with the deposition of  $150nm$  of polymethyl methacrylate (PMMA) electron beam resist, followed by electron-beam lithography to define structures in PMMA. We use an  $Ar^+$  ion milling step to transfer the mask pattern through the Au metal mask, and this procedure is followed by a  $C_2F_6$  reactive ion etching (RIE) to transfer the mask from the Au into the SiON. Inductive-coupled plasma RIE (ICP RIE) etching is finally used to transfer the pattern from the SiON mask layer into the InGaAsP. Finally, the mask is removed in a HF solution and the InGaAsP membrane is released from the substrate by wet etching in 4:1 HCl:water solution at  $4^\circ C$ . The final structure is a free standing membrane supported at one side (Figure 2). Each pattern, shown in Figure 2(a), consists of six different cavities that have received the same electron-dose during the e-beam lithography step, and therefore they should have similar hole size ( $r$ ) and lattice constant ( $a$ ). The only difference is the value of the elongation parameter  $p$  that assumed values in the range  $p/a \in (0, 0.25)$ . The periodicity of the structure characterized here was  $a = 435nm$  and the hole radius  $r = 138nm$ . This combination of geometries lead relative thickness of  $d/a = 0.759$  and relative hole size  $r/a = 0.317$ . Using three-dimensional finite difference time domain code (3D FDTD), we have found that in this case, the photonic bandgap is located in the range

$$a/\lambda = (0.253, 0.345).$$

The structures were optically pumped using  $10 \div 30$ ns long pump pulses (periodicity  $1\mu s$ ) from semiconductor laser diode ( $\lambda_{pump} = 830nm$ ). The pump beam was focused through 100x objective lens onto the sample surface to obtain a spot size of about  $3\mu m$ . The emission from the cavities is collected through the same lens, and the spectrum of the emitted light signal is detected with an optical spectrum analyzer (OSA). An additional flip-up mirror is used to obtain the optical images of the excitation pump-spot and the cavity modes.

As the first step we have measured the emission from the unprocessed InGaAsP material and obtained the gain spectrum of the active material. We have found that emission exists between 1300nm and 1650nm, with a maximum at around 1550nm. This wavelength range corresponds to normalized frequencies of  $a/\lambda \in (0.264, 0.335)$ , which is within the bandgap of the bulk photonic crystal mirrors surrounding the cavity. Next, we have tested all six cavities (Figure 2) in order to measure their resonant modes. We have found two prominent resonant peaks in the emission range of our InGaAsP material, and observed that these two modes are linearly polarized, but have orthogonal polarization (Figure 3). This is in an excellent agreement with our 3D FDTD analysis that shows that two orthogonally polarized modes (LQ polarized along y- and HQ along x-axis) exist in this wavelength range (Figure 3). We have also found that the position of these resonances depends strongly on the value of the elongation parameter  $p$  (Figure 4), as predicted in our earlier publication<sup>8</sup>. Moreover, theory predicts that the mode at longer wavelengths (HQ) should have much higher Q values than the one at shorter wavelengths (LQ). This was confirmed in our experimental measurements, and  $Q \approx 2,000$  was found in the case of HQ mode ( $p_5$  cavity), while Q of only several hundreds was measured in the case of LQ mode.

As the next step we tested our devices for lasing, using pump pulses with a microsecond periodicity. Poor thermal heat sinking was expected for our membrane resonators, since the free standing membranes are attached to the substrate at only one side. Thus, we have pumped with limited duty cycles to  $< 3\%$ . Lasing was observed in our cavities for several  $p_4$  and  $p_5$  structures, with different  $r/a$  parameters and defect hole sizes. In some cases lasing

could also be observed in  $p_3$  cavities. This appears to be in contradiction with our theoretical prediction that  $p_2$  and  $p_3$  structures should have the highest Q factors and smallest mode volumes, and therefore the lowest threshold powers. However, structures with higher  $p$  parameter also have more gain due to increased amount of active material in the cavity. Therefore, it is not surprising that lasing was much readily observed in the case of more elongated geometries with  $p_5$  than in  $p_3$  devices. In Figure 5 we show the L-L curve for one of the lasing photonic crystal nanocavities. Threshold powers as low as  $P_{th} = 214\mu W$  were observed when this laser was pumped with 1% duty cycle. To the best of our knowledge, this is the smallest threshold power observed in photonic crystal cavities, and certainly the lowest pump power for a laser with a highly localized mode. Quality factors in the case of  $p_5$  structure was estimated from below threshold luminescence measurements to be around  $Q \approx 2,000$  (Figure 5), and these are in good agreement with theoretical predictions. Unfortunately, we were not able to obtain reliable estimates for Q factor values in the case of  $p_2$  and  $p_3$  cavities due to the weak emission from these devices below threshold. However, according to theoretical predictions, we expect these cavities to have Q factors as high as 10,000. Yoshie et al.<sup>10</sup> have analyzed very similar devices in quantum dot material and have obtained Q factors of about 2,800. However, these devices incorporate a slightly different type of edge dislocation, and thus the predicted Q factors from Yoshie's devices were limited to about 4,000.

In Figure 6 we show the L-L curve for a laser structure with an elongation  $p_4$ . In addition to the elongations, the holes are smaller in this structure ( $r/a = 0.292$ ) than in the lasers described above. This cavity was again found to support two modes, and the one at longer wavelength also has the higher Q factor which lases. A photoluminescence spectrum taken above threshold, as well as the mode profiles taken at different pumping levels, are shown in the inset. It can be seen that the lasing peak is very well localized in the center of this cavity, and also resembles the slightly ellipsoidal profile characteristic for the high Q mode expected from a cavity with a fractional edge dislocation(see Figure 4). Moreover, the size of the measured light spot is observed to be on the order of  $3.9\mu m^2$ , a strong indication

that this laser has a small mode volume. When the pump beam is only slightly moved from the center of the cavity (less than  $1\mu\text{m}$ ), the strong light intensity shown in Figure 6 disappears. This microluminescence pumping result is another confirmation that we indeed observe lasing from a well localized, small mode volume, high Q resonant mode.

In conclusion, we have observed room temperature lasing from high Q cavities based on fractional edge dislocations in triangular lattice planar photonic crystals. Lasing is observed from the high Q dipole mode of this nanocavity. In spite of the unusual design of our structures, which have a hole etched through the position of maximum field intensity and therefore reduced overlap with gain material, we observe low threshold powers in our devices. We have attributed this to the small mode volume and the high Q factors inherent to our device design. In addition, the low Q dipole mode, positioned at shorter wavelengths, is experimentally detected and matches our finite difference time domain model predictions. Polarization and lithographic tuning properties of high- and low-Q modes are also in an excellent agreement with theoretical FDTD predictions. The mode profile taken by our IR camera shows that the lasing resonance is well localized to the center of our cavity. Based on these experimental results, we conclude that the observed lasing corresponds to the high Q mode of our fractional edge dislocation cavity.

This work was sponsored by Caltech MURI center for Quantum Networks.

↑  
IPL<sub>1</sub> <sup>support</sup> acknowledgement will be added  
- Paula Quevedo

## REFERENCES

- <sup>1</sup> E. Yablonovitch, *Phys. Rev. Lett.*, 58, 2059 (1987).
- <sup>2</sup> T. F. Krauss, R. M. De La Rue and S. Brand, *Nature*, 383, 699 (1996).
- <sup>3</sup> O. J. Painter, A. Husain, A. Scherer, J. D. O'Brien, I. Kim and P. D. Dapkus, *J. of Lightw. Tech.*, 17, 2082 (1999).
- <sup>4</sup> H. G. Park, J. K. Hwang, J. Huh, H. Y. Ryu and Y. H. Lee, *Appl. Phys. Lett.*, 79, 3032 (2001).
- <sup>5</sup> P. T. Lee, J. R. Cao, S. J. Choi, Z. J. Wei, J. D. O'Brien and P. D. Dapkus, *IEEE Phot. Tech. Lett.*, 14, 435 (2002).
- <sup>6</sup> H. Y. Ryu, S. H. Kim, H. G. Park, J. K. Hwang, Y. H. Lee, *Appl. Phys. Lett.*, 80, 3883 (2002).
- <sup>7</sup> C. Monat, C. Seassal, X. Letartre, P. Viktorovitch, P. Regreny, M. Gendry, P. Rojo-Romeo, G. Hollinger, E. Jalaguier, S. Pocas and B. Aspar, *Elec. Lett.*, 37, pp. 764-766 (2001).
- <sup>8</sup> J. Vučković, M. Lončar, H. Mabuchi and A. Scherer, *Phys. Rev. E.*, 65, 016608 (2001).
- <sup>9</sup> J. Vučković, M. Lončar, H. Mabuchi and A. Scherer, to appear in *IEEE Journal of Quantum Electronics*.
- <sup>10</sup> T. Yoshie, J. Vučković, A. Scherer, H. Chen and D. Deppe, *Appl. Phys. Lett.*, 79, 4289 (2001).

## FIGURES

FIG. 1. (a) Conventional single defect cavity ( $p = 0$ ). When structure is "cut" along the dashed line, and two PPC half-planes are dislocated along  $\Gamma X$  direction by  $p/2$ , (b) high-Q cavity can be formed ( $p = 0.25 \cdot a$ ).

FIG. 2. (a) Six different cavities with elongation parameters  $p_0 = 0$ ,  $p_1 = 0.05 \cdot a$ ,  $p_2 = 0.1 \cdot a$ ,  $p_3 = 0.15 \cdot a$ ,  $p_4 = 0.2 \cdot a$  and  $p_5 = 0.25 \cdot a$ . (b) Blow-up of  $p_3$  cavity

FIG. 3. Polarization dependance of the two modes detected in the  $p_3$  cavity, obtained using polarizer positioned at different angles with respect to  $y$ -axis direction ( $0^\circ$  - polarization along  $y$ -axis). Figure also shows mode profiles ( $B_z$  component) and polarization ( $\vec{E}$  field) of the LQ and HQ modes, the result of 3D FDTD analysis.

FIG. 4. Position of resonant modes detected in cavities  $p_0 \div p_5$  as a function of the elongation parameter  $p$ .

FIG. 5. L-L curve for  $p_5$  cavity for two different duty cycles (DC). The pulse periodicity was  $1\mu s$  in both cases. Spectrum taken below threshold (arrow) is shown in the inset.

FIG. 6. L-L curve for  $p_4$  cavity that also incorporate smaller holes ( $r/a = 0.292$ ). Lasing action occurs at  $\lambda = 1598nm$ . Insets show spectrum above threshold, and mode profiles of the lasing mode for several pump levels. The boundaries of the structure can also be seen. The mode is very well localized to the center of the cavity.

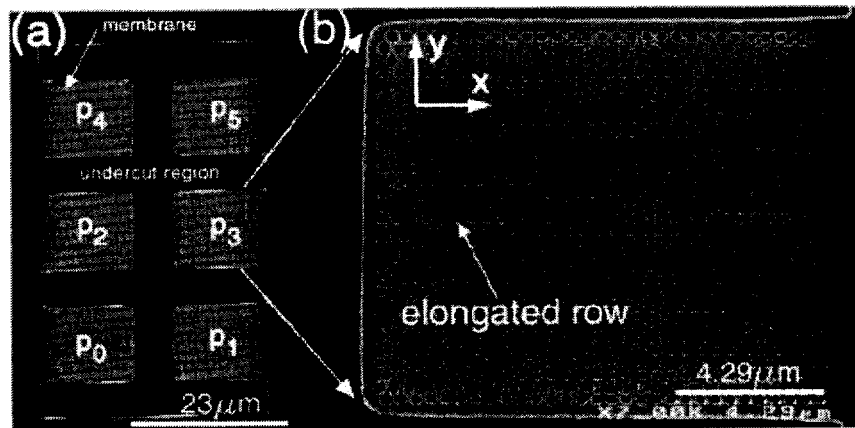


Figure 2

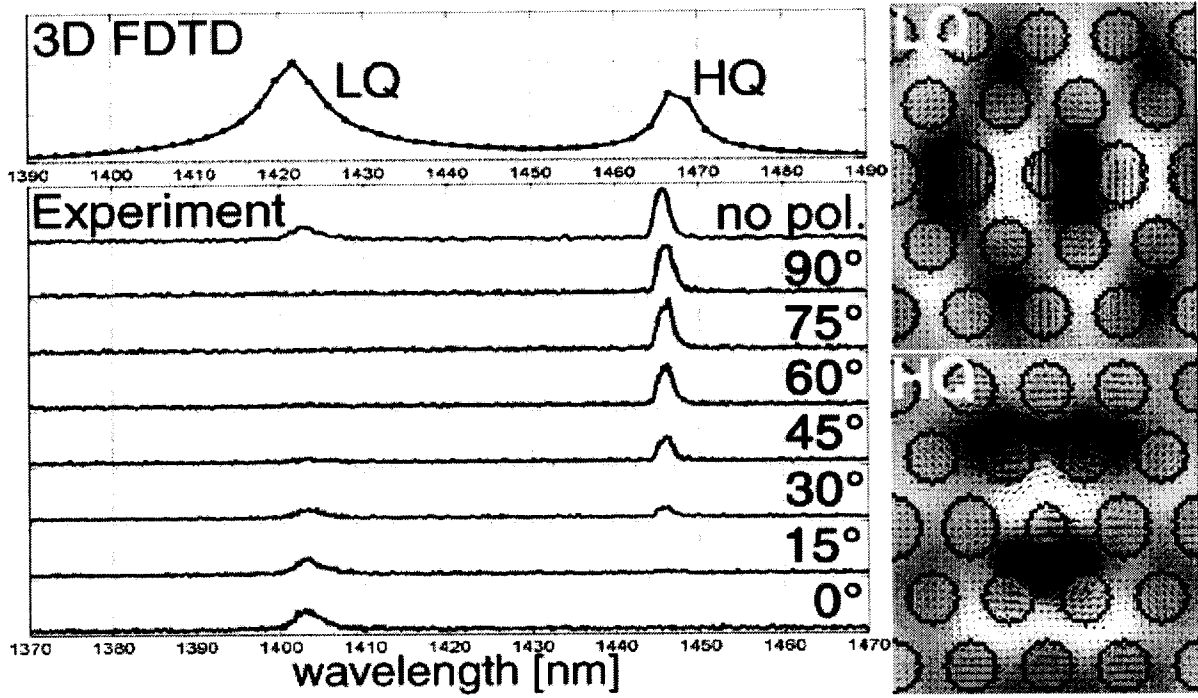


Figure 3

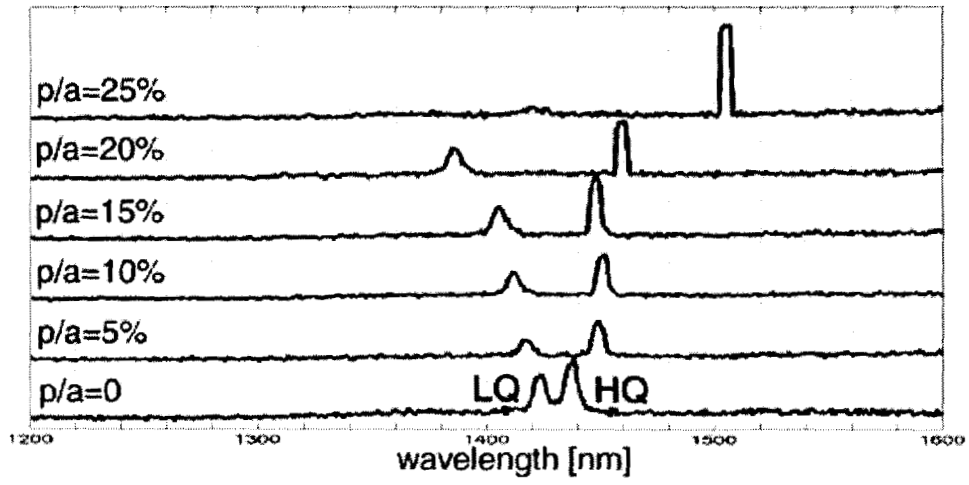


Figure 4

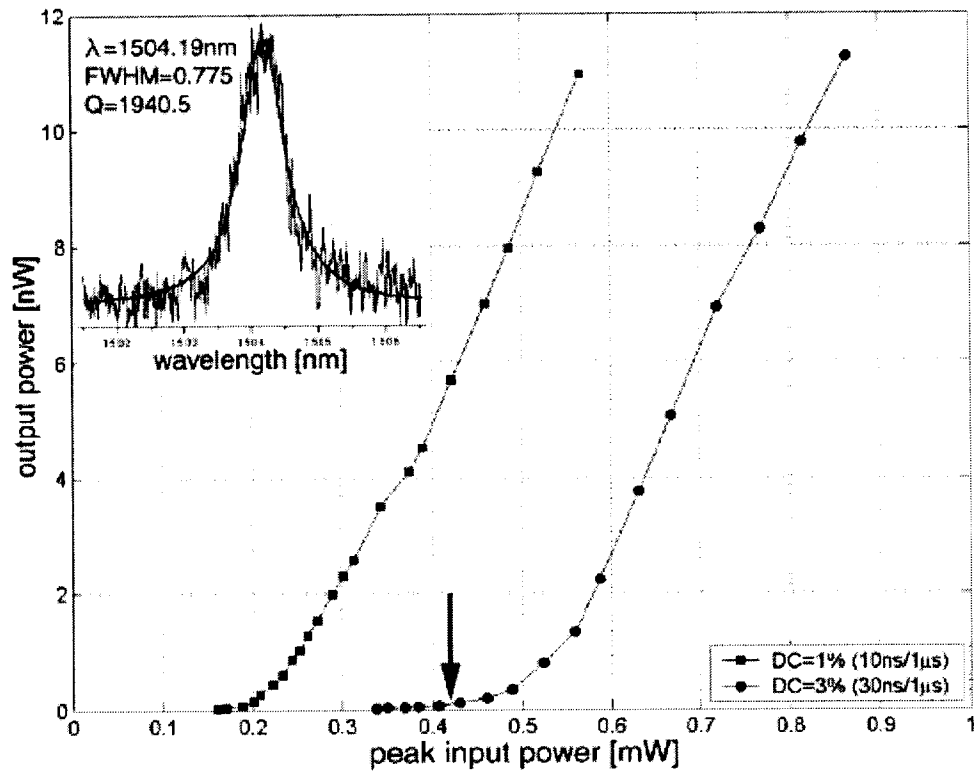


Figure 5

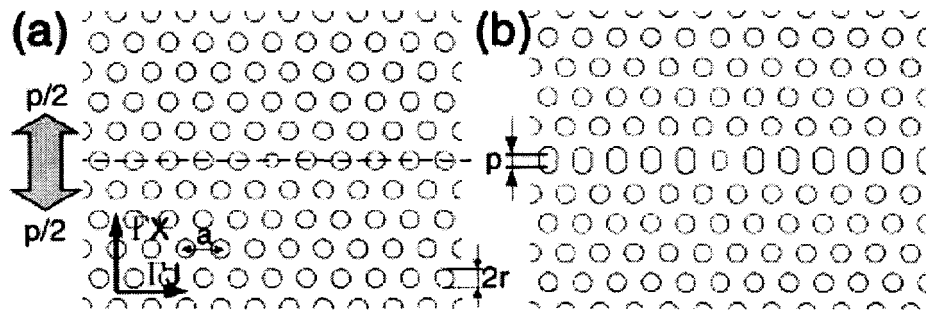


Figure 1

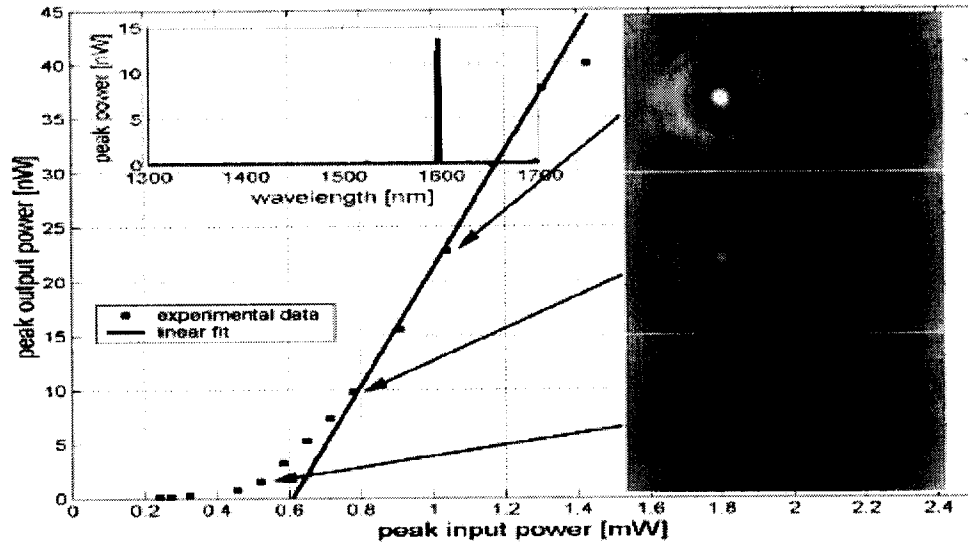


Figure 6